Numerical Study on a Passive Micromixer with Sinusoidal Channel Walls

Arshad Afzal[*] and Kwang-Yong Kim[**]

[*,**] Department of Mechanical Engineering,
Inha University, Incheon, 402-751, Rep. of Korea**,** kykim@inha.ac.kr

ABSTRACT

A computational study is carried out for a passive micromixer with wavy channel walls of sinusoidal variation for Reynolds numbers in the range $0.1 \leq Re \leq 30$. A mixing index is used to evaluate the performance of the micromixer. The mixing performance showed a strong dependence on the wavelength of the sinusoidal walls over the entire Re range considered. A shift in the center of rotation of Dean vortices toward inner sinusoidal wall for lower wavelength mixers was found to be an important factor significantly affecting the chaotic mechanism at higher Re. For a fixed mixing length, the sinusoidal design showed a remarkably improved mixing performance compared to a square-wave channel. This micromixer can easily be realized and integrated with microfluidic systems due to its simple in-plane structure.

Keywords: microfluidics, micromixer, Dean vortices, chaotic mixing.

1 INTRODUCTION

Mixing of liquid samples in microfluidic systems has attracted many researchers mainly due to small characteristic dimensions of the channels and absence of turbulence. Micromixers can be divided into two broad categories: active and passive. The active types require complex fabrication procedures and are difficult to incorporate with micro systems. In contrast, passive micromixer uses the geometry of the device to produce complex flow field for effective mixing. Depending on the mode of operation, different realizations of passive micromixers have been developed. A typical passive method to enhance the mixing process was proposed by Stroock *et al.* [1] using bas-relief structures on the floor of a channel. The patterned topography can be used to generate transverse flow that increases the interfacial area between the fluids to be mixed.

For flows through curved and bended channels, secondary flows evolve as a result of inertial and centrifugal effects. Liu *et al.* [2] studied mixing in a 3-D serpentine microchannel for a wide Reynolds number range of $6 \leq Re \leq 70$. Mixing in the serpentine channel was found to depend on the secondary flows originating at the bends. Howell *et al.*[3] showed the formation of Dean vortices by directing flow through a curved channel of square cross-section. Jiang *et al.* [4] used such secondary flows to induce chaotic mixing for flows through meandering channels. Vanka *et al.* [5] carried out a computational study to determine mixing rates in a curved square duct at low Reynolds numbers. Thus, there has been significant research on the generic problem of mixing via curved conduits.

Numerical simulation using computational fluid dynamics (CFD) have been carried out for a passive micromixer with sinusoidal walls proposed by Afzal and Kim [6]. With wavelength as the geometrical parameter, the micromixer is investigated for a wide Reynolds number range $0.1 \leq Re \leq 30$. Mixing index is employed to evaluate the performance of the micromixer.

2 PROBLEM DEFINITION AND QUANTIFICATION OF MIXING

A diagrammatic layout of the problem is given in Fig. 1. The profile of the main channel was generated using a sine function of the form $y = A \sin(2\pi x / \lambda)$ where A is the amplitude, λ is the pitch or wavelength, and x and y are the spatial coordinates. The value of A was taken to be 0.2 mm.

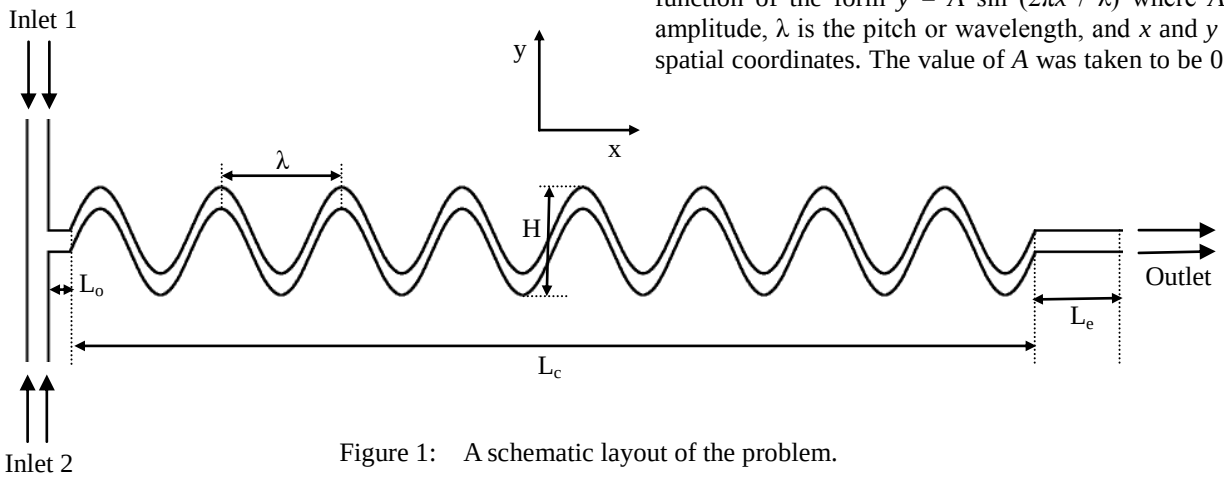

Figure 1: A schematic layout of the problem.

The two sine curves have offset-y = 0.1 mm; i.e., the distance between any two opposite points on the respective curves is 0.1 mm. The value of H is 0.5 (= 2a + 0.1) mm. The depth of the channel is 0.1 mm. The two inlets, Inlet 1 and Inlet 2, having a square cross-section dimension of 0.1 mm × 0.1 mm, are merged to the main channel with a T-joint as shown in Fig. 1. The axial lengths of the connecting channel L_o and exit channel L_e are fixed at 0.1 and 1.8 mm, respectively. The length of main channel L_c is a function of wavelength for a fixed mixing length. Simulations were carried out using ANSYS CFX-11 [7], a commercial computational fluid dynamics (CFD) package based on the finite volume method. The numerical analysis was carried out by solving the steady 3-D Navier-Stokes equations and advection-diffusion-type equation for the concentration field with appropriate boundary conditions.

$$\vec{\nabla}.\vec{V} = 0 \tag{1}$$

$$(\vec{V}.\vec{\nabla})\vec{V} = -\frac{1}{\rho}\nabla p + \nu\nabla^2\vec{V} \tag{2}$$

$$(\vec{V}.\vec{\nabla})C_i = \alpha\nabla^2 C_i \tag{3}$$

where $\vec{V}$ represents the fluid velocity, ρ and v are fluid density and kinematic viscosity, α is the diffusivity coefficient and C_i is the concentration respectively. The properties of the working fluids, Ethanol and water, were measured at 20 ℃ [8].

Hexahedral cells were used to discretize the computational domain. Using grid-independence test, a grid size of 3×3×3 μm was found to be accurate for spatial resolution. The SIMPLEC algorithm was used for pressure-velocity coupling. Multigrid techniques were used to accelerate the convergence behavior. The prediction accuracy of the numerical methods used in our study has been proven in previous works [9] for mixing in various micromixers. A variance-based method was employed to evaluate the mixing performance of the micromixer. The variance of the mass fraction of the mixture on a cross-sectional plane normal to the flow direction can be expressed mathematically as

$$\sigma = \sqrt{\frac{1}{N}\sum_{i=1}^{N}(c_i - c_m)^2} \tag{4}$$

where N is the number of sampling points on the plane, c_i is the mass fraction at sampling points i, and c_m is the optimal mixing mass fraction. Finally, the mixing index at any cross-sectional plane perpendicular to the axial direction is defined as

$$M = 1 - \sqrt{\frac{\sigma^2}{\sigma_{max}^2}} \tag{5}$$

Where σ_{max} is the maximum variance over the range of data. A higher value of M (close to 1) indicates a better mixing quality.

3 RESULTS AND DISCUSSION

For flows through curved conduits with circular or rectangular cross-sections, centrifugal force acts on fluid particles as a result of fluid inertia and curvature. However, fluid particles moving along the centerline experiences a higher centrifugal force (maximum axial velocity)

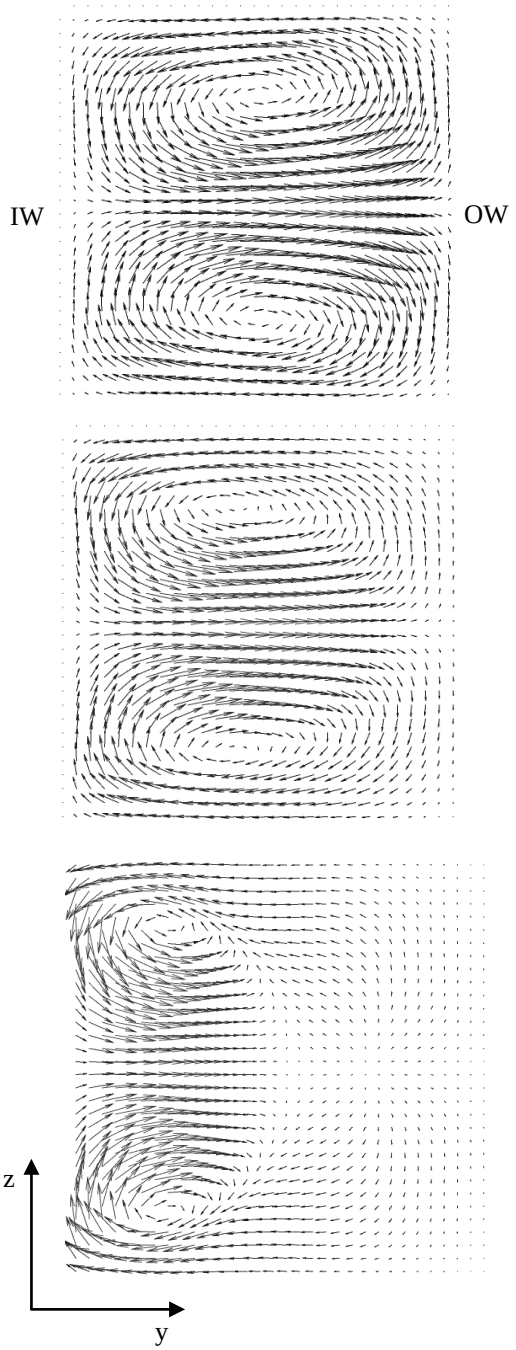

Figure 2: Secondary flows on the cross-sectional planes located at Peak for λ = 1.12 mm (left), 0.56 mm (middle), and 0.28 mm (right). IW and OW denote the inner and outer sinusoidal walls respectively.

compared to the particles near the wall. On account of differential centrifugal forces, secondary flows are set up in the cross-sectional plane of the channel characterized by the presence of two-counter rotating vortices (known as Dean's vortices) [10]. The Dean number κ, is defined as $Re(d/R)^{1/2}$, where d is the characteristic cross-sectional dimension of the channel and R is the radius of curvature. Dean number (κ) gives an idea of the intensity of the secondary motion. Two major aspects of the sinusoidal design of the micromixer are: Firstly, the turns at the highest (peak) and lowest (trough) points induce curvature to the path of the flow. Consequently, Dean vortices appear at the cross-sectional plane located at peaks and troughs for the entire range of Reynolds number. The direction of rotation of the vortices is reversed at the Troughs due to change in the sign of curvature. The vortex pair existed even when the Reynolds number was very small. However, at very low flow rates (Re ≤ 1), secondary flows are rather weak to perturb the interface and mixing is mainly by diffusion between adjacent concentration layers. As the strength of secondary flow increases with increasing Reynolds number (Re >10), interface modulation commonly known as stretching and folding occurs, thereby increasing the mixing above the diffusive limit. As the pitch was decreased, the radius of curvature at the turns was reduced, although not in a proportional manner. Thus, it is suggested that the intensity of the secondary flow increases with decreasing pitch for a fixed Re. Secondly, the sinusoidal design offers a simple narrowing of the channel geometry in the nearly-straight parts due to the inherent nature of the sine function. Thus, the proposed arrangement minimizes the diffusion distance. The diffusion rate was significantly improved for lower wavelength micromixers as a result of the corresponding lowering of the diffusion distance. Fig. 2 shows Dean vortices in terms of velocity vector plots on a cross-sectional plane located at the peak for different wavelengths. It was observed that the center of rotation of the vortex is shifted towards the inner channel wall with decreasing wavelength. To provide an explanation for the shift in the center of rotation with wavelength, trends in the velocity profile is exploited. Local velocity is normalized by the respective average flow velocity and plotted against the normalized channel width as shown in Fig. 3 [6]. With parabolic velocity profile, the maximum velocity occurs at the center of the channel, and thus, the fluid moving down the center experiences a higher centrifugal force than the fluid near the walls. For λ = 1.12 mm, the centre of rotation is nearly located at the midpoint of the respective vortices owing to the parabolic flow profile. For lower wavelengths, however, the maximum velocity position shifts towards the inner sinusoidal wall and the flow profile remains no longer parabolic. Therefore, the centre of rotation of Dean vortices moves towards the inner sinusoidal wall as dictated by the differential centrifugal forces. As the fluid travels from peak to trough, the change in channel curvature inverts the rotational direction of the vortex. The shift in the vortex center towards the inner sinusoidal wall for the lower wavelength mixers (λ = 0.56 and 0.28 mm) results in the vortices centered at opposite positions on cross-sectional planes located at peaks and troughs, respectively. This asymmetry induces strong chaotic flow. Fig. 4 shows effect of wavelength on mixing performance at Re = 30 with number of turns (Odd and even numbers represent peaks and troughs respectively). For λ = 1.12 mm, the change in the sign of channel curvature at the trough inverts the rotation direction of the vortices. Thus, for one complete cycle, the effect on interface modulation was neutralized and mixing was very

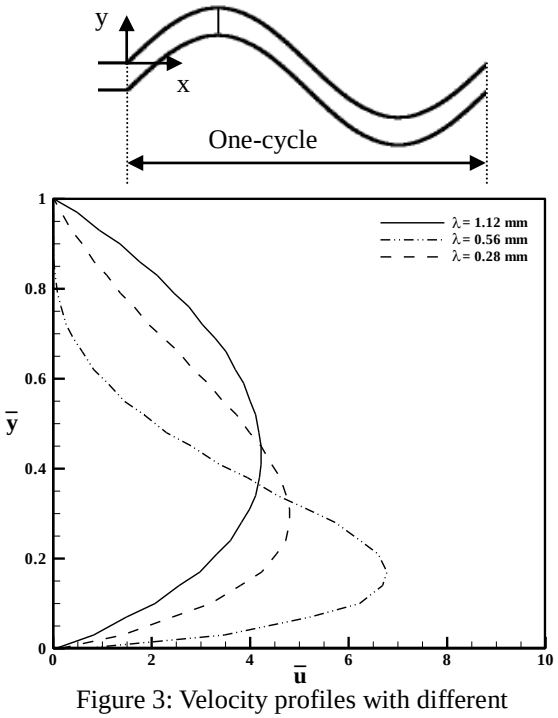

Figure 3: Velocity profiles with different wave lengths for Re = 30(lower and upper limits denote the inner and outer sinusoidal walls respectively) [6].

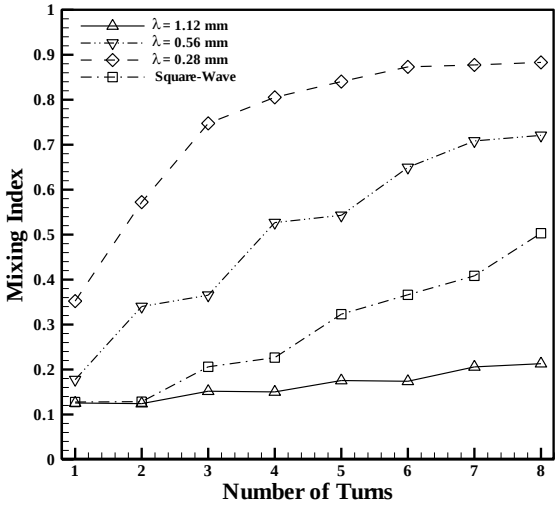

Figure 4: Variations of mixing index with number of turns.

slow. However, lower wavelength channels (λ = 0.56 and 0.28 mm) present advantage of the stronger and asymmetric Dean vortices resulting in enhanced mixing.

Fig. 5 shows mixing performance as a function of mixing length for three different wavelengths at Re = 0.5. For Re $\leq$ 1, the secondary flow was weak and mixing was primarily by diffusion. Thus, for a similar path length traversed by the co-flowing fluids, a lower wavelength micromixer demonstrated a significantly improved performance due to reduction in diffusion distance in the channel cross-section. The mixing performance was evaluated in comparison to a square-wave channel of comparable dimensions (λ = 0.28 mm) for Re = 0.5 and 30. The proposed sinusoidal mixer demonstrates significantly improve performance for both low and high Reynolds numbers (Fig. 4 and 5).

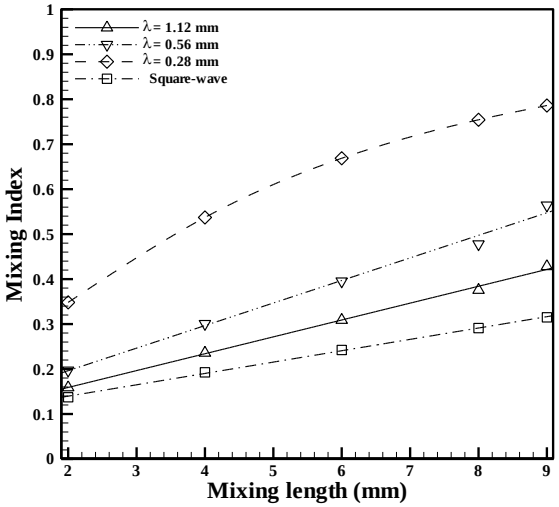

Figure 5: Mixing index for Re = 0.5 as a function of mixing length.

Fig. 6 shows the results obtained by the previous work [6] for the mixing performance of the micromixer for a wide Reynolds number range, 0.1 $\leq$ Re $\leq$ 30. The fluid in the micromixer travel curved paths, therefore, a fixed mixing length was used for comparison at different wavelengths. Mixing was primarily by diffusion for Re $\leq$ 1. Since, diffusive mixing is affected by the residence time of the fluid in the channel; the mixing quality deteriorates with increased Reynolds number at a fixed design wavelength. At higher Reynolds numbers (Re >10), interface modulation known as stretching and folding occurs on account of secondary flow leading to increased area for diffusion and the mixing performance was significantly improved. However, due to weak secondary flow at Re 10 for λ = 1.12 mm, the mixing was primarily diffusion dominated. Although the mixing index is same for λ = 0.56 and 0.28 mm (Re = 30) for a fixed mixing length, lower wavelength generates stronger secondary flow and mixing progresses relatively fast utilizing fewer number of turns (Fig. 5).

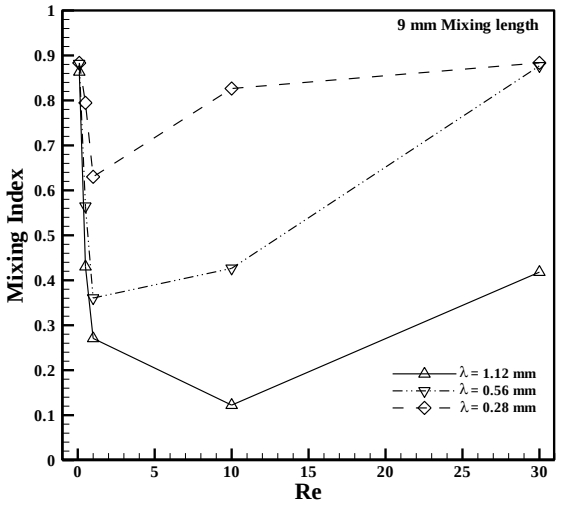

Figure 6: Variations of mixing index at the exit with Reynolds number for different wavelengths [6].

4 CONCLUSIONS

Numerical simulation based on Navier-stokes equations are carried out for a passive micromixer with sinusoidal walls for Reynolds number in the range 0.1 $\leq$ Re $\leq$ 30. The mixing performance is found to sensitively increase as the wavelength of the sinusoidal channel walls decreases over the entire Re range considered. A different chaotic mixing mechanism with a shift in the centre of rotation of Dean vortices towards inner sinusoidal wall was observed for lower wavelength microchannels. The sinusoidal design showed superior mixing performance compared to a square-wave channel for both diffusive and chaotic regimes.

REFERENCES

[1] A. D. Stroock, S. K. W. Dertinger, A. Ajdari, I. Mezic´, H. A. Stone and G. M. Whitesides, Science 295, 647, 2002.
[2] R. H. Liu, M. A. Stremler, K. V. Sharp, M. G. Olsen,J. G. Santiago, R. J. Adrian, H. Aref and D. J. Beebe, J. Microelectromech. Syst. 9, 190, 2000.
[3] P. B. Howell, Jr., D. R. Mott, J. P. Golden and F. S. Ligler, Lab Chip 4, 663, 2004.
[4] F. Jiang, K. S. Drese, S. Hardt, M. Küpper and F. Schönfeld, AIChE J. 50, 2297, 2004.
[5] S. P. Vanka, G. Luo and C. M. Winkler, AIChE J. 50, 2359, 2004.
[6] A. Afzal and K. Y. Kim, Chem. Eng. Res. Design, submitted, 2012.
[7] CFX-11.0, Solver Theory, ANSYS, 2007.
[8] S. Hossain, M. A. Ansari and K. –Y. Kim, Chem. Eng. J. 150**,** 492, 2009.
[9] M. A. Ansari and K. Y. Kim, Chem. Eng. Sci. 62, 6687, 2007; AIChE J. 55, 2217, 2009.
[10] W. R. Dean, Philos. Mag. 4**,** 208 (1927); Philos. Mag. 5**,** 673, 1928.